

# The new SANS instrument at the Swiss spallation source SINQ

Joachim Kohlbrecher\* and Werner Wagner

Paul Scherrer Institut, CH-5232 Villigen PSI, Switzerland.  
E-mail: joachim.kohlbrecher@psi.ch

With the start-up of the neutron spallation source SINQ at PSI an instrument for small angle neutron scattering became operational and is open for the user community. The instrument is equipped with state-of-the-art components and compares well with the world's largest and most powerful facilities of this kind. Great emphasis was put on providing a flexible, universal multi-user facility which guarantees a comfortable and reliable operation. In the present paper, the layout of the instrument is presented, the main components are described, and the performance is illustrated by selected examples.

## 1. Introduction

Since September 1998 the new instrument for Small Angle Neutron Scattering (SANS) (PSI SANS website, 1999) is in user operation at the continuous spallation source SINQ at PSI. The design of the SINQ-SANS instrument follows the classical concept of the D11-instrument at the ILL, Grenoble (Ibel, 1976). Installed at a cold neutron guide, it uses in its basic configuration a mechanical velocity selector for monochromatization, and a straight pin-hole collimation system for the primary beam tailoring. Behind the sample, in the secondary flight path, a two-dimensional position sensitive detector is used to register the neutrons scattered around the primary beam. Aside from the velocity selector (which is placed inside the bunker), the instrument is assembled in the guide hall of the SINQ, stretching to a total length of about 40 m with a secondary flight path of up to 20 m.

## 2. The individual components

### 2.1. Neutron beam and wavelength selection

The neutron guide, facing the cold D<sub>2</sub>-moderator at its entrance, is curved to filter epithermal and higher energy neutrons. Coated with isotopically enriched <sup>58</sup>Ni in the curved section, its lower cut-off wavelength ("characteristic wavelength") is 0.42 nm. The cross-section is a square of 50 × 50 mm<sup>2</sup>.

Inside the bunker, the guide has a gap of 43 cm in which the beam shutter, a primary beam monitor, and the mechanical velocity selector are placed. We have chosen the Dornier velocity selector (Wagner et al., 1992), rotating at a maximum speed of 28300 rpm for neutrons of 0.45 nm wavelength and with a rotor length of only 25 cm. The standard wavelength spread is 10% (FWHM). By tilting the selector relative to the neutron beam direction this value can be decreased to 8% (tilting -10°) or increased up to 20.6% (tilting +10°).

### 2.2. Collimation

The collimator allows for the adjustment of the collimation length, i.e. the distance between the two pinholes at the guide exit and at the specimen position, in discrete steps between 1 m and 18 m which then matches the *Q*-resolution chosen by the sample-detector distance. Mechanically, this flexibility is achieved by a system of eight collimator segments between 1 m and 4 m long, mounted in sequence

with vacuum-tight connections. Each section is a revolving device with three tubes. One of the tubes is always filled with a neutron guide, the second one, lined with shielding material, carries apertures for beam tailoring and absorption of parasitic radiation. The third one either carries special elements or is empty. The lengths of the segments are such that the exit of the closest neutron guide can be placed at 1 m, 1.4 m, 2 m, 3 m, 4.5 m, 6 m, 8 m, 11 m, 15 m and 18 m from the sample. For the 1 m distance, a focusing neutron guide ("antitrompete") in the last collimator segment allows an increase of the neutron flux on the specimen in the high *Q* – low resolution configuration. The aperture sizes at the beginning and at the end of the collimation system can be freely chosen up to the cross-section of the neutron guide of 50 × 50 mm<sup>2</sup>.

### 2.3. Detection

The secondary flight path is enclosed by steel vacuum tube with a diameter of 2.7 m. It houses a two-dimensional <sup>3</sup>He multiwire proportional counter with a sensitive area of 96 × 96 cm<sup>2</sup> and 128 × 128 detection elements of 7.5 × 7.5 mm<sup>2</sup> each. The detector is mounted on a rail-guided trolley such that it may be positioned with its detection plane at any distance between 1.50 m and 20 m from the sample. Further, an increase of the *Q*-range at any detector distance can be achieved by an optional lateral displacement of the detector of up to 50 cm, combined with a rotation around the central vertical axis of the detector to minimize parallax effects.

The detector electronics (preamplifier, amplifier, logic units etc.) is entirely mounted on its rear in a volume which is at atmospheric pressure and connected to the outside by a series of flexible tubes which run cables and a cooling air flow. The maximum count-rate of the detector is specified with 20 kHz per pixel and 200 kHz for the whole detector. Immediately in front of the detector, a beamstop of B<sub>4</sub>C-plates is mounted on a thin-walled aluminium tube, moveable in vertical and horizontal direction. Four beamstops of dimensions 40 × 40 mm<sup>2</sup>, 70 × 70 mm<sup>2</sup>, 85 × 85 mm<sup>2</sup> and 100 × 100 mm<sup>2</sup> are available and may be exchanged by remote control in the vacuum.

### 2.4. Histogram memory

The detector electronics is connected to a programmable histogram memory which is equipped with sufficient memory to store 64 detector images. The histogram memory has a trigger input and 6 address channels over which the sample environment can directly address the image index under which the detected neutrons will be stored. This allows dynamic and cyclic experiments with time constants in the milliseconds to minutes range.

### 2.5. Performance

The momentum transfer *Q* which corresponds to a given spot on the detector is given by  $Q = 4\pi/\lambda \sin(\arctan(r/D)/2)$ , where  $\lambda$  is the neutron wavelength, *r* the radial distance of the spot from the beam center, and *D* the sample-to-detector distance. If we assume that the closest distance to the beam center at which reliable data may be recorded is  $r_{min} = 5$  cm, which is half the size of the largest beam stop, then the minimum in *Q*-range at *D* = 20 m and  $\lambda = 2$  nm is  $Q_{min} = 8 \times 10^{-3}$  nm<sup>-1</sup>. The maximal *Q* at *D* = 1.5 m and  $\lambda = 0.45$  nm with the detector centered to the beam axis ( $r_{max} = 48$  cm) is  $Q_{max} = 4.3$  nm<sup>-1</sup> or, for a 50 cm lateral detector displacement ( $r_{max} = 96$  cm)  $Q_{max} = 8$  nm<sup>-1</sup>.

The neutron flux at the sample position has been measured by standard gold foil activation, and by using a <sup>3</sup>He-detector of 100 % efficiency (diameter 5cm, pressure 5 bar) at the sample position (Wagner et al., 1998). The flux data measured for various collimation distances *D* and wavelengths  $\lambda$  ( $\Delta\lambda/\lambda = 0.1$  FWHM) are shown in Fig. 1. They

are multiplied with the square of the collimation distance to scale them to a common solid angle of the beam divergence. The scaling is excellent except for small wavelengths ( $\lambda < 0.8$  nm) at the 2 m position. In this configuration, the beam is undercollimated, i.e. the collimation is given by the full divergence of the guide. The flux values at 1 mA compare favourably with those of other instruments of the same type. They equal within  $\pm 10\%$  the flux at the sample position of the SANS-instrument of HMI, Berlin and are about a factor 3 below the D11-instrument at the ILL in Grenoble. (Note that we expect a flux increase by a factor of about 2 from an improved second generation SINQ target, which at present is under construction.)

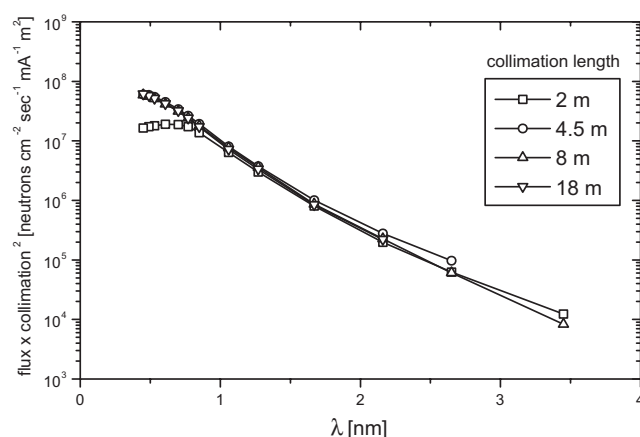


**Figure 1** Neutron flux scaled to the squared collimation distance, as a function of neutron wavelength for different collimation lengths. Resolution of the mechanical velocity selector:  $\Delta\lambda/\lambda = 0.1$  FWHM. For the flux measurement the full cross-section of the neutron guide of  $50 \times 50$  cm and a diaphragm of 10 mm in diameter in front of the  $^3\text{He}$  detector has been used.

## 2.6. Sample environment

To satisfy the large variety of experimental needs of the users we gave high priority to a maximum versatility of the sample environment. One standard set-up is a sample table with  $x, y, z, \omega$  positioning plus an optional  $(\theta, \phi)$ -goniometer. On this table various sample environment set-ups can be mounted and positioned. For biological and chemical samples a sample changer is provided for cuvettes and solid samples which can be temperature controlled between  $-40^\circ\text{C}$  and  $+150^\circ\text{C}$ . A high pressure cell for liquids up to 5 kbar is under construction and, in collaboration with the ETH Zürich, a high temperature furnace operating at up to  $1500^\circ\text{C}$  is being build. Together with the University of Birmingham (UK) a cryomagnet with a field of up to 11 Tesla in the horizontal direction with a geometry optimized for SANS, has been ordered and will be available next year.

A second sample environment set-up is a vacuum chamber, directly connected to the collimator and detector tubes, such that the SANS can be operated at about  $10^{-2}$  mbar in a single vacuum system without windows. If better vacuum down to  $10^{-6}$  mbar or ambient pressure is needed at the sample position, it is possible to insert thin aluminium or sapphire windows at the entrance and exit of the chamber. The chamber is large enough to house a 1.5 Tesla electromagnet combined with a vertical sample changer with an optional heated sample position for temperatures up to  $750^\circ\text{C}$ . Instead of the heated sample holder the electromagnet can also be combined with a closed cycle cryostat, so that measurements down to 8 K are possible.

## 2.7. Alignment System

For a fast alignment of the sample behind the beam defining aperture a light optical system is implemented. A silicon wafer, transparent for neutrons, mounted at about 0.8 m in front of the sample position acts as a mirror for light from either a halogen lamp or a laser, both mounted outside the evacuated collimation tube behind a quartz window. This light beam is aligned in a way that it follows the axis of the neutron beam, illuminating the sample in its correct position.

## 2.8. Data acquisition and software

The SANS instrument is controlled by the SINQ instrument control software SICS (Könnecke et al., 1997) developed at the PSI. SICS is a client server system with the SICS server providing the functionality of the instrument and the clients implementing user interfaces. SICS is designed for maximum portability, easy configuration and extendability. The immediate benefit of a client server model is that clients can be distributed across multiple computer platforms and only the server has to run on a defined workstation. This model allows an easy control of all components of the instrument from any computer at which the clients (written in Java) are installed. The measured data are stored by the server program in the NeXus data format standard (PSI NeXus website, 1999) (Könnecke et al., 1996). For the primary data reduction the BerSANS software package from HMI Berlin (Germany) has been adapted to our instrument.

## 3. Concluding remarks

In the first half year of the instrument's operation already a large variety of experiments have successfully been performed by users: Investigations of flux lattices in superconductors, in situ measurements on decomposition in alloys, investigations of pores and porosities in ceramics, relaxations in holographic gratings, interparticle arrangements of colloidal suspensions, etc.

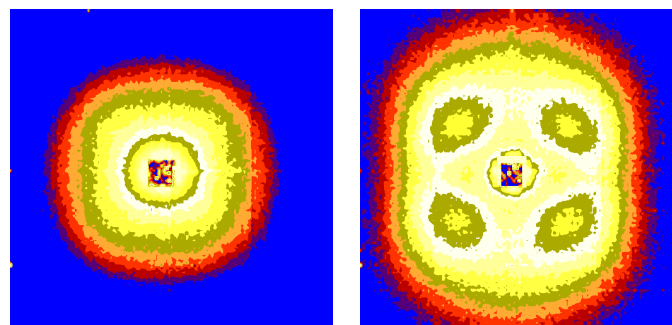


**Figure 2** SANS intensity of the two-phase magnetic alloy Cu-24at.%Ni-8at.%Fe after annealing at 823 K for 967h, measured in zero field (left) and in a horizontal external magnetic field of 4.5 kOe (right) ( $Q$ -range 0.02 - 0.2 nm $^{-1}$ ). The picture at the right indicates an anisotropic distortion of the magnetic SANS intensity.

As an example Fig. 2 shows intensity maps of the annealed ternary alloy Cu-24at.%Ni-8at.%Fe (SINQ experimental reports website, 1999), which upon annealing establishes a two phase morphology where ferromagnetic precipitates are embedded in a nonmagnetic matrix. In zero field, the scattering is found isotropic (Fig. 2 left), indicating on average a nearly random distribution of the magnetization vectors of the precipitates. For non-zero fields the scattered intensity becomes highly distorted and shows a pronounced anisotropy of four-fold symmetry.

### References

- [http://www1.psi.ch/www\\_sinq\\_hn/SINQ/instr/sans.html](http://www1.psi.ch/www_sinq_hn/SINQ/instr/sans.html)
- Ibel, K. (1976). *J. Appl. Cryst.* **9**, 296–309.
- Wagner, V., Friedrich, H., & Wille, P (1992). *Physica B* **180&181**, 938–940.
- Wagner, W., Bauer, G.S., Duplich, J, Janßen, S., Lehmann, E., Lüthy, M., & Spitzer, H (1998). *J. Neutron Res.* **6**, 249-278.
- Könnecke, M. & Heer, H., (Dubna, Russia 1997). *International workshop on data aquisition systems for neutron experimental facilities (DANEF'97)*, 265–279.
- <http://ins00.psi.ch/NeXus/index.html>
- Könnecke, M. & Arends, P., (1996). *J. Neutron Res.* **4**, 9–14.
- [http://www1.psi.ch/www\\_ins\\_hn/SINQ/ER/II\\_98S\\_32.pdf](http://www1.psi.ch/www_ins_hn/SINQ/ER/II_98S_32.pdf)